

5th Workshop on Metallization for Crystalline Silicon Solar Cells

Basic study on the influence of glass composition and aluminum content on the Ag/Al paste contact formation to boron emitters

S. Körner^{*,a}, F. Kiefer^b, R. Peibst^b, F. Heinemeyer^b, J. Krügener^c, M. Eberstein^a

^aFraunhofer IKTS, Winterbergstr. 28, 01277 Dresden, Germany

^bInstitut für Solarenergieforschung GmbH Hameln/Emmerthal Am Ohrberg 1, 31860 Emmerthal, Germany

^cInstitute of Electronic Materials and Devices, Leibniz Universität Hannover, 30167 Hannover, Germany

Abstract

In this study, the contact formation of aluminum containing silver metallization pastes for boron emitters was investigated. Model pastes with varied glass composition (PbO-containing and PbO-free) and Al content were prepared. It was found, that glass viscosity as well as Al content have a strong influence on densification behavior of the pastes. The most significant effect of the aluminum addition is the change of the thermodynamic conditions in the system silver-glass-silicon. For investigations of the contact formation an in-situ-contact resistance measurement was performed. The interface morphology of the pastes in dependence on the firing temperature was investigated by means of cross section samples in SEM and EDX. Finally, n-type Si solar cells were electrically characterized and the IV-data were correlated to the interface morphology.

© 2015 The Authors. Published by Elsevier Ltd. This is an open access article under the CC BY-NC-ND license (<http://creativecommons.org/licenses/by-nc-nd/4.0/>).

Peer-review under the responsibility of Gunnar Schubert, Guy Beaucarne and Jaap Hoonstra

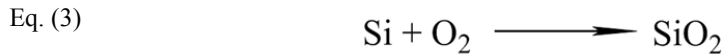
Keywords: n-type solar cell; front-side metallization; glass viscosity; aluminum content; in-situ-contact resistance

1. Introduction

According to the International Technology Roadmap for Photovoltaic, monocrystalline n-type silicon is predicted to gain a share of the Si-based PV market up to ~39% until 2024 [1]. N-type material offers several advantages over p-type silicon, e.g. the absence of light induced degradation, higher bulk lifetimes and insensitivity to common metal impurities. A promising candidate for a “step-stone” from today’s screen-printed aluminum-BSF cells is the PERTL (Passivated Emitter Rear Totally (Locally) doped) cell concept with screen-print metallization of the boron front-side emitter [2-4]. It can be fabricated via a lean process flow, which is, in many steps, similar to that of today’s p-type cells.

The contact formation of glass containing silver pastes was been studied by various authors [5-8]. During firing in a RTP (rapid thermal processing) furnace, the glass addition in the paste becomes liquid and dissolves some Ag as

Ag₂O. If the glassy interface gets in touch with the Si_xN_y:H ARC (anti reflection coating) layer and the silicon, Ag₂O is reduced immediately to Ag according to equation 1. The driving force of this reaction can be found in the Gibb's free energy. For the reaction according Eq. 2, the free energy becomes positive at temperatures higher than 200 °C. In the meanwhile, Gibb's free energy for the oxidation of silicon (Eq. 3) is at elevated temperatures negative (e.g. at 800 °C ΔG = -708 kJ/mol).



By these metallic silver precipitations in between the silicon wafer and the silver layer are formed, which provides electrical conductivity of the interface. The reaction intensity, namely the amount of the Ag precipitations and the amorphous glass layer thickness, are crucial for the electrical performance of the solar cells.

However, the formation of the contact between screen-printed front-side metallization and boron emitters is technologically challenging due to specific interactions with a glass containing silver paste [9]. It has been found that the addition of aluminum to silver pastes is advantageous to achieve a reasonably low specific contact resistance ρ_c [10, 11]. Nevertheless, the contact formation mechanism and the role of Al is still not fully understood in the community.

Commercial contact pastes feature a number of ingredients inhibiting the study of detailed reaction mechanisms [11, 12]. For our investigation, model pastes with simplified recipes are used. The type of glass frit is varied to study the influence of the glass frit chemistry. Additionally the aluminum content on the sintering behavior and contact formation was studied. For investigations of the contact formation an in-situ-contact resistance measurement was performed. The interface morphology of the pastes in dependence on the firing temperature was investigated by means of cross section samples in SEM and EDX. Finally, n-type Si solar cells were electrically characterized and the IV-data were correlated to the interface morphology.

2. Experimental

Model pastes containing 95-x Vol% silver, 5 Vol% glass frit and x Vol% aluminum (x = 0; 2.5; 7.5 Vol%) were prepared at IKTS. One lead-oxide containing (glass A) and one lead-oxide- and bismuth-oxide-free glass (glass B) frit was tested. The action of these two glasses in the contact formation on p-type wafers was recently reported [13]. The glasses show a different temperature-viscosity-behavior. Viscosity measurement of the glasses was conducted by observation of the silhouette of a glass powder pressing (diameter and height of 2 mm) in a Hot Stage Microscope (Leica Wetzlar Germany) using a heating rate of 10 K/min. Typical sample shapes can be related to glass viscosity fix points (sinter onset – $\eta = 10^{8.6}$ Pa s, final sinter point – $\eta = 10^{6.8}$ Pa s, minimal point – $\eta = 10^{4.4}$ Pa s, hemisphere point – $\eta = 10^{2.8}$ Pa s, flow point – $\eta = 10^{2.0}$ Pa s) [14].

For each silver-glass-composition the aluminum addition amount according to Table 1 was varied. As organic binder system ethyl cellulose (5 wt%) dissolved in terpeneol and dibutyl phthalate was used. The pastes were homogenized on a three-roll mill to give good dispersion as well as similar viscosity and printing behavior.

As cell architecture, the PERT technology was chosen. Preparation of the 156mm×156mm monocrystalline pseudo-square cell precursors was performed at ISFH. The pastes were screen printed on a 70Ω/□ boron front-side emitter passivated by an Al₂O₃/Si_xN_y stack. For printing, a screen with 70μm wide finger openings and an emulsion over mesh (EOM) thickness of 15μm was used. After drying, the cells were fired in a standard PV infrared belt furnace from Centrotherm. The peak firing temperature was varied: 780°C, 810°C and 840°C. After local ablation of the Si_xN_y passivation on the phosphorus doped cell rear-side by a picosecond laser, thermal evaporation of aluminum was performed in a high-throughput inline evaporation tool from Applied Materials.

Table 1: Composition of the model pastes (Vol%)

Paste	Glass A PbO containing	Glass B PbO free	Silver	Aluminum
1	5		95	0
2	5		92.5	2.5
3	5		87.5	7.5
4		5	95	0
5		5	92.5	2.5
6		5	87.5	7.5

The characterization of the light-IV, dark-IV and J_{sc} - V_{oc} curves at standard testing conditions was performed at ISFH utilizing a LOANA cell tester from pvtools. Polished cross sections of the finger regions from solar cells were prepared at ISFH. SEM and EDX measurements were performed at ISFH utilizing a Hitachi SEM system.

For measurement of the in-situ-contact resistance a test structure was printed at the IKTS. Firing of these test structures was performed at the three peak temperatures which yielded the highest efficiencies on cell level. During firing, the contact resistance was measured in-situ with a home-build setup (IKTS). For this purpose, a data logger (Q18, Datapaq Ltd.) was used for a quasi-4-point probes method. So far, this experimental setup allows no normalization, so absolute values are obtained. For an interpretation of the contact formation mechanism, focus lies at the shape of the resistance curve. They are discussed in detail in Sec. 3 in comparison to results from previous studies on p-type wafers [8].

3. Results

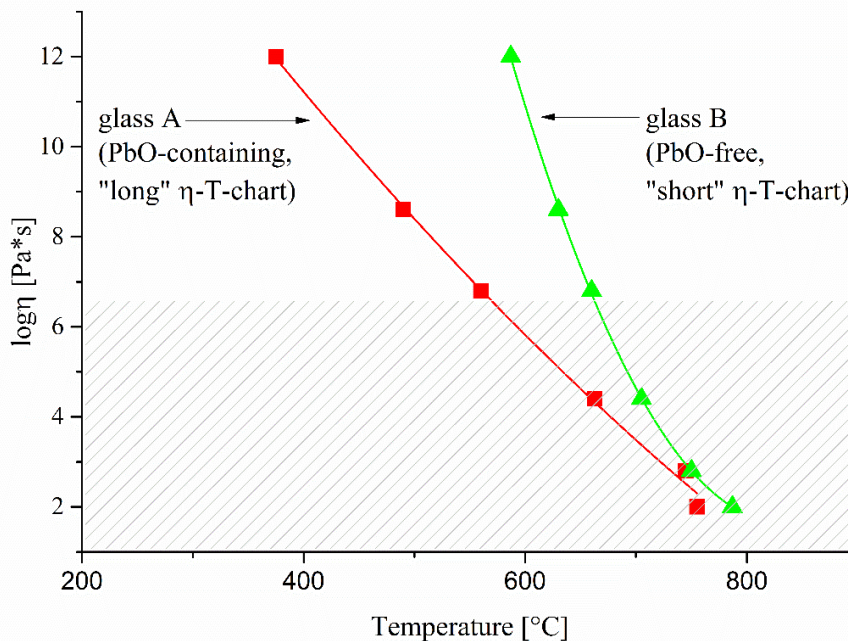


Figure 1: Viscosity as function of temperature for both glasses used in this study. Glass A – red squares, Glass B – green triangles. Hatching indicates the viscosity range, in which the glass melt is electrical conductive [9].

In Figure 1, the viscosity as function of the temperature is shown for both glasses used. The lead-oxide containing glass A has a low softening temperature of 568 °C and a “long” character, which means that softening of the frit happens during a broad temperature interval. Compared to this, glass B softens at 665 °C and has a “short” character (steep slope of viscosity change during heating). Therefore, the softening occurs in a smaller temperature regime. Both glasses have a similar viscosity at temperatures higher than 700 °C. The hatched area indicates the temperature in which the glasses have a viscosity lower than $10^{6.6}$ Pa*s (related to the glass softening point T_{soft}). In this range, glass melts have ionic mobility and are capable of conducting electrical current [15].

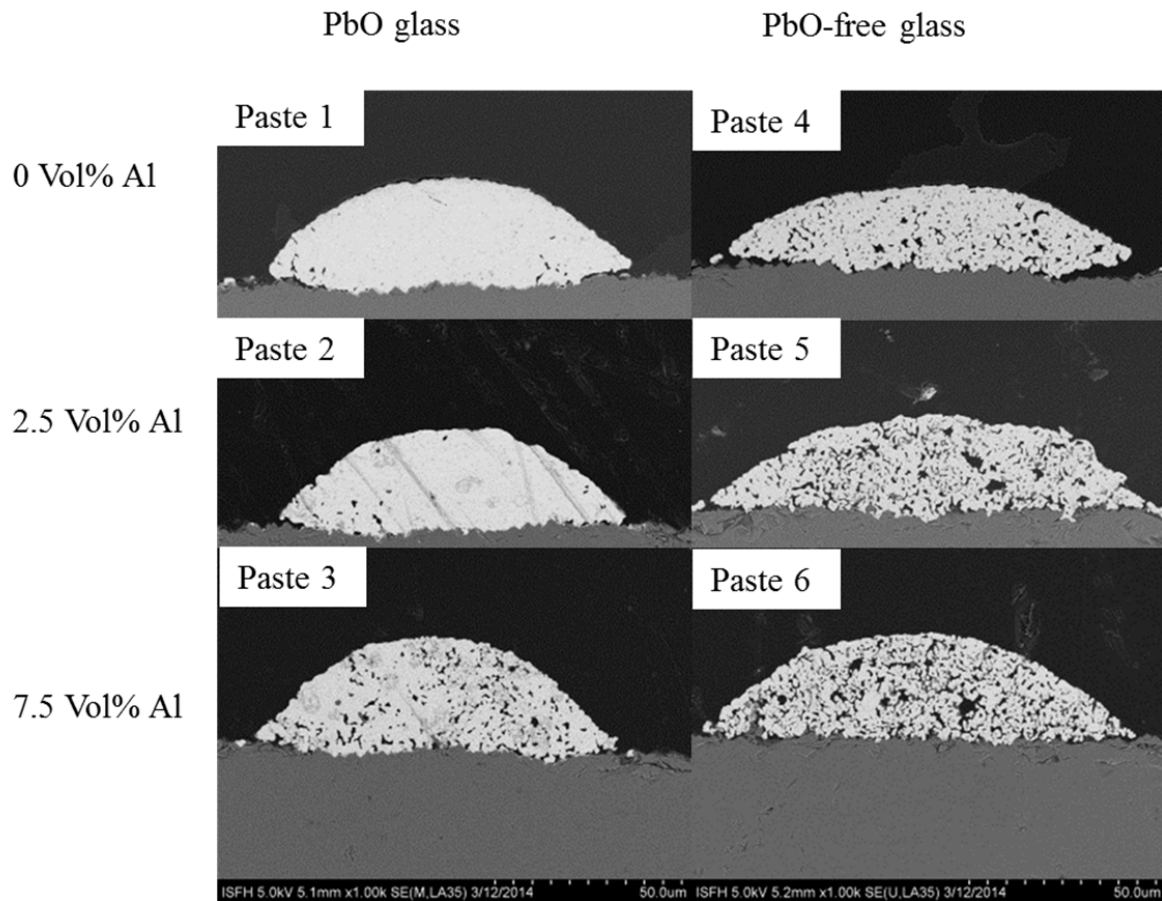


Figure 2: Polished cross sections of grid line fingers of the pastes according to Table 1 in dependence of Al content. Left column – pastes with glass A, right column – pastes with glass B. Increasing aluminum content from 0 Vol% (top row) up to 7.5 Vol% (bottom row). Peak firing temperature was 810°C; magnification 5000x.

Figure 2 shows polished cross sections of fired gridline fingers obtained from the different pastes. The densification of the model pastes used varies with the glass frit and the Al content. The peak firing temperature was 810°C. Using glass A and no Al addition in paste 1, it shows almost complete densification of the finger microstructure. This correlates with the long viscosity character of glass A (softening point at ~560°C) and resulting relatively long action of liquid phase during the sintering. By contrast, substitution of glass A by glass B yields a higher porosity. Glass B has a short character and the softening of the glass starts at temperatures higher than ~670°C. Therefore, the liquid phase is formed at higher temperatures and can only give support over a shorter time scale to the densification of the silver powder.

With the addition of 2.5 Vol% aluminum (middle row) the porosity is increased for both pastes (paste 2 and 5). This trend continues with the addition of 7.5 Vol% aluminum which implies a significant porosity in the silver-glass-compositions (paste 3 and 6). The sinter densification seems retarded by the presence of Al additions in both silver-glass-compositions.

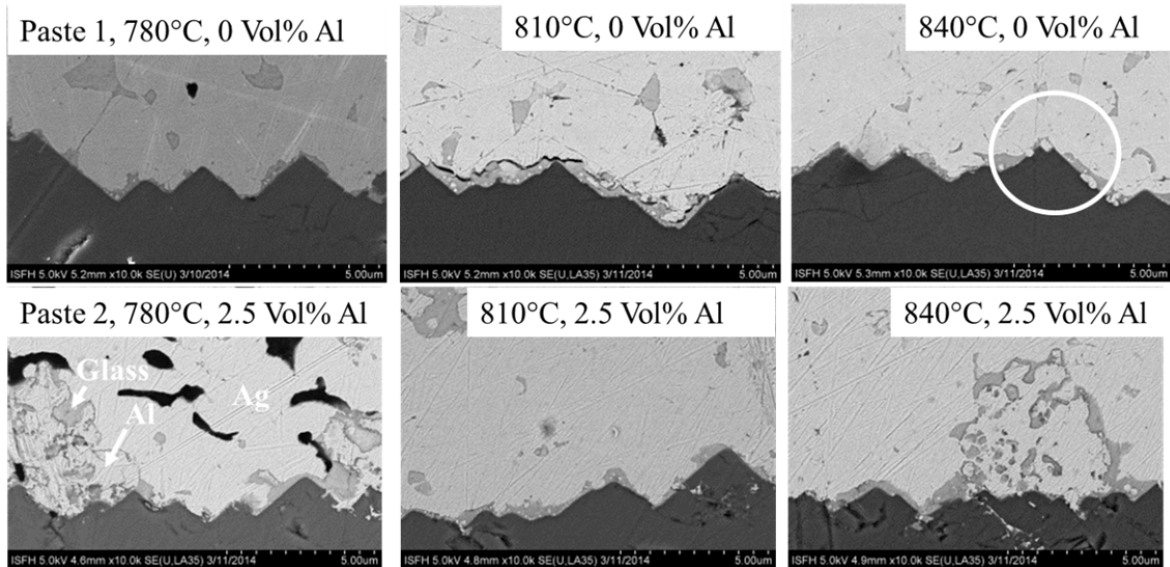


Figure 3: Polished cross sections of grid line fingers of pastes according to Table 1 in dependence of firing temperature. Paste 1 – top row and paste 2 – bottom row; Magnification 10 000x.

In Figure 3 the contact interfaces for paste 1 (top row) and paste 2 (bottom row) in dependence of peak firing temperature are shown. For paste 1, fired at the lowest temperature, an amorphous interface layer is observable (paste 1, 780°C). The glassy layer is thin ($< 1 \mu\text{m}$) and spread over large parts of the surface. At regions with thicker glassy layer, silver precipitations can be recognized. With increasing peak firing temperature, the amorphous layer becomes thicker and more inhomogeneous (Paste 1 – 810°C). The amount of silver in the amorphous layer increases. For the highest temperature (Paste 1 – 840°C) even some silver precipitations grown in the wafer surface are present (indicated by white circle).

Adding 2.5 Vol% Al (Paste 2, Figure 3 – bottom row) to the paste, the appearance of the cross section changes dramatically. The interface of paste 2 in dependence on firing temperature features a remarkable inhomogeneous glass layer. The former Al grains obviously have been subjected to a reaction during firing which results in a glass-aluminum-conglomerate appearance. Between the Al and the Si wafer, the glass layer is somewhat depleted and it contains only few silver precipitates. With increasing temperatures (Paste 2 – 840°C), the amount of silver in the amorphous layer as well as its thickness is increased. The vicinity of the former Al grain contains more glass. For further insights in the phase distribution, EDX analysis was performed (Figure 4).

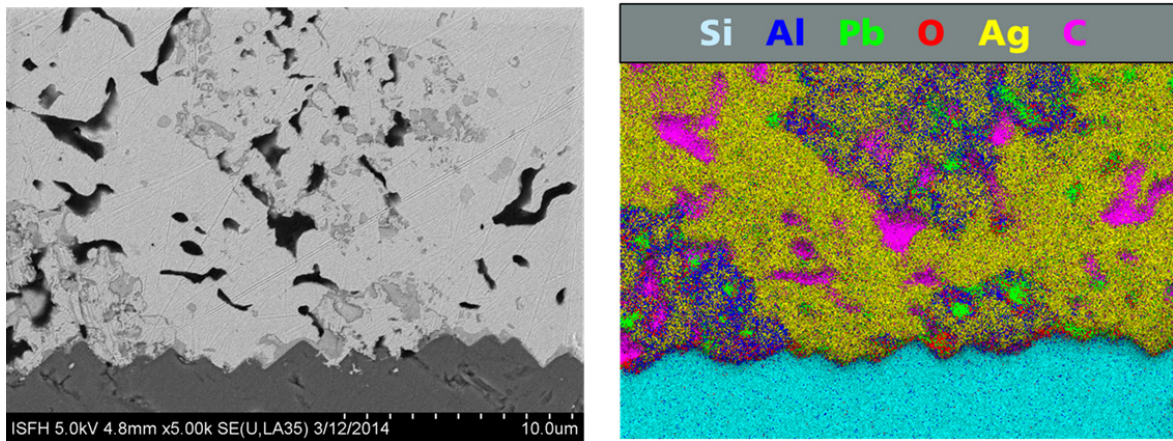
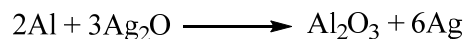


Figure 4: Polished cross section of a metallization finger of paste 2 (PbO containing glass frit, Al content 2.5 Vol%) fired at 780 °C peak firing temperature. Left – SEM image; right – EDX analysis of the same sample.

Figure 4 shows an exemplary SEM cross section image (left hand side) of the metal-silicon interface and the corresponding EDX analysis image (right hand side) for paste 2 (low viscous PbO-containing glass frit, Al content 2.5 Vol%, fired at 780 °C). In the EDX false color image, it is possible to distinguish between the silver (yellow) and aluminum (blue). It is obvious, that in the areas of the former Al grain silver can be found. Lead (green) and oxide (red) as indicator for the glass frit are additionally preferential in the vicinity of Al than in the pure silver bulk material.

The most significant effect of the aluminum addition is the change of the thermodynamic conditions in the system silver-glass-silicon. The oxidation of silicon to equation 3, which is energetically preferred in common aluminum-free pastes, is partly oppressed by the reaction according to equation 4, which has still lower Gibb's free energy. This leads to a realignment of the silver containing glassy liquid phase in the vicinity of the Al-grains at the expense of the thickness of the glassy interface layer. The consequences are a lower sintering densification rate and a lower reaction intensity in the paste-wafer interface. Another effect of the Al in the paste is a decreasing amount of silver in the amorphous interface layer. At the wafer surface it is reduced with silicon because the SiO₂ formation has a significant lower Gibb's Free Energy. However, the Gibb's Free Energy for the formation of Al₂O₃ (Eq. 4) is even lower (-892 kJ/mol) and the reduction of silver oxide with Al is energetic convenient over the reduction of silver oxide with silicon. With these two aspects, less silver is transported to the Si wafer.

Eq. (4)



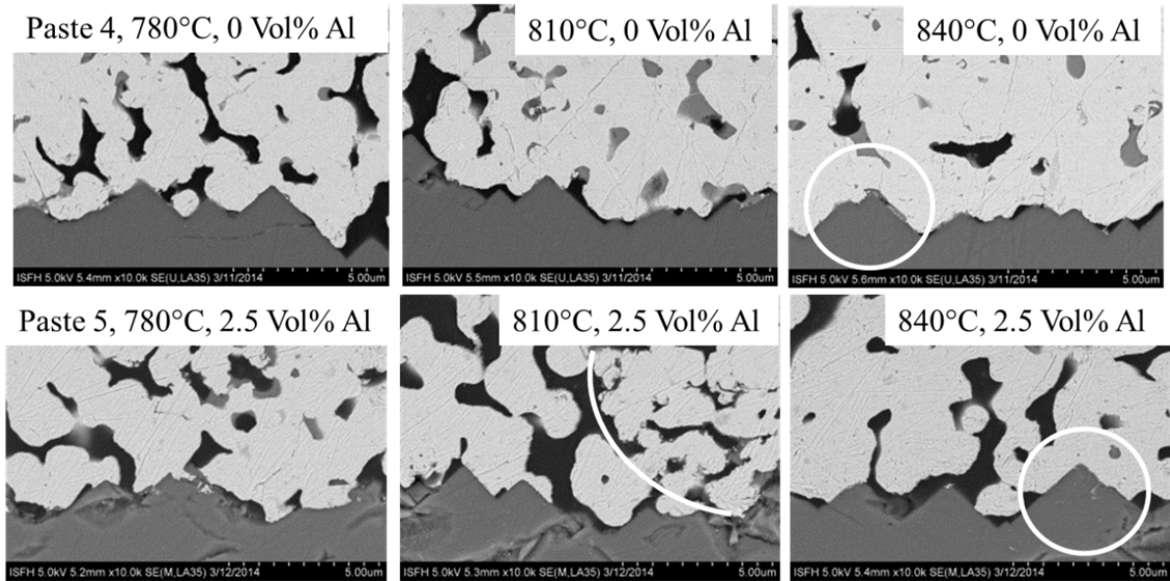


Figure 5: Polished cross sections of grid line fingers of pastes according to Table 1 in dependence of firing temperature. Paste 4 – top row and paste 5 – bottom row; Magnification 10 000x.

In Figure 5 cross sections of the contact interface from paste 4 (top row) and paste 5 (bottom row) are shown. The interface of paste 4 shows a completely different image compared to paste 1. The glass layer between silver and silicon is very thin but features some silver precipitations (Paste 4 – 780°C/810°C). At some regions there seems to be a direct silver silicon contact (Figure 5 – top row, 840°C indicated by white circle). With increasing firing temperature the amorphous layer thickness and its amount of silver is increased. However, there is no silver grown in the wafer surface, as in the case of paste 1 (Figure 3 – top row, 840°C). Only nano sized silver precipitations are observed. With the addition of Al (paste 5 – Figure 5, bottom row) the contact interface becomes inhomogeneous. The wafer surface seems to be roughened by Si diffusion like described in [9]. In the surrounding of the Al conglomerate (indicated by white semicircle Figure 5 – bottom row, 810°C) there is no strong glass enrichment like for the lead-oxide containing glass A. The amorphous interface layer is thinner as for paste 4 without Al. In the white circle Figure 5 (bottom row, 840°C) an area with a mixture from ultrathin glass layer (not visible in this magnification) and direct Ag-Si-contact is indicated. In addition, there can be observed some small spikes from the silver metallization towards the silicon. For a time resolved investigation of the contact formation process, in-situ-resistance measurements were performed.

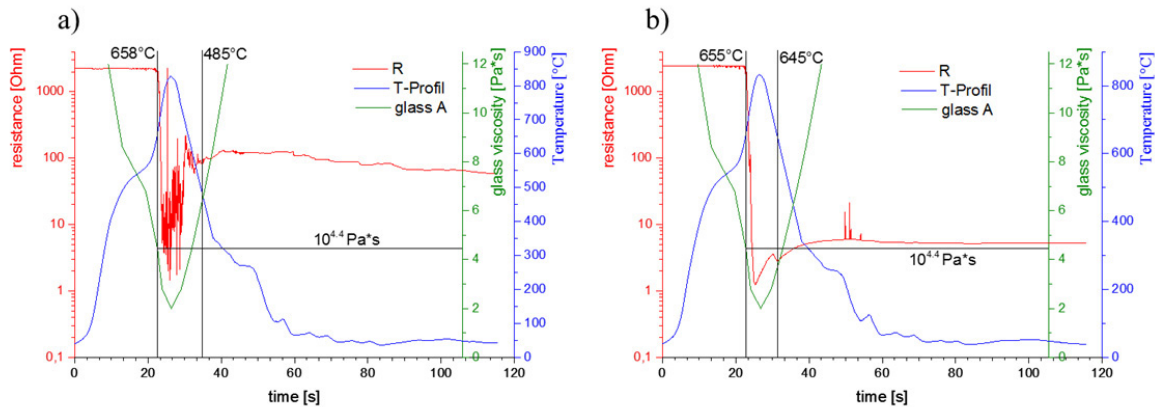


Figure 6: Contact resistance during as a function of time contact firing at 840°C of paste 1 (PbO containing glass A, without Al – left hand side) and paste 3 (PbO containing glass A, 7.5 Vol% Al – right hand side) as function of time. Red curve – contact resistance; blue curve – temperature; green – glass viscosity of glass A related to the temperature plot.

Figure 6a shows the contact resistance as a function of time for paste 1 (glass A, without Al). Before reaching the peak firing temperature of 840°C at about 27 s, the resistance drops at 650–680°C from values higher than 1000 Ohm down to values low than 10 Ohm. After this first drop, the resistance scatters with a high amplitude. After passing the peak firing temperature at 35 s and undercutting a temperature of 485°C the scattering vanishes. However, the resistance shows a slight increase up to about 100 Ohm. The final resistance after complete cool down at 100 s the final resistance is about 67 Ohm. Firing paste 2 (glass A, 7.5 Vol% Al; Figure 6b) at 840°C, the resistance drops also at temperature between 650–660°C. By contrast to paste 1, in the peak range no scattering of the resistance occurs. Shortly after passing the peak range the resistance increases and attains the end resistance of 5 Ohm (100 s).

Comparing the in-situ-contact resistance measurements at paste 1 and paste 2 it is obvious that the first resistance drop for both pastes starts in the same temperature range 655–658°C, which correlates with a glass viscosity of about $10^{4.4}$ Pa*s (see Figure 1). Since the aluminum oxide / silicon nitride stack (ARC) at the top of the wafer is an insulating layer, the drop of the resistance indicates the opening of this layer by an electrical conduction liquid glass phase, which confirms results in [13]. Within this picture, the fact that the resistance drops for both pastes occurs in the same temperature range, indicates that the opening of the ARC depends on the glass viscosity. The scattering after the resistance drop can be handled as indicator for the intensity of the convection processes in the amorphous interface layer due to the redox reaction [16]. The scattering of the resistance in the peak range can be found only for paste 1 (without Al). Adding Al to the paste, this scattering is smoothed. Obviously, this is a consequence of the fact that the amount of glass at the interface decreases (see figure 3 – bottom row). Significant amount of glass is located in the Al-glass-conglomerate. Glass which is bounded in vicinity of the Al agglomerates is not available for the interface reaction and therefore does not contribute to the contact formation. This is indicated by the smooth resistances curve (Figure 6b).

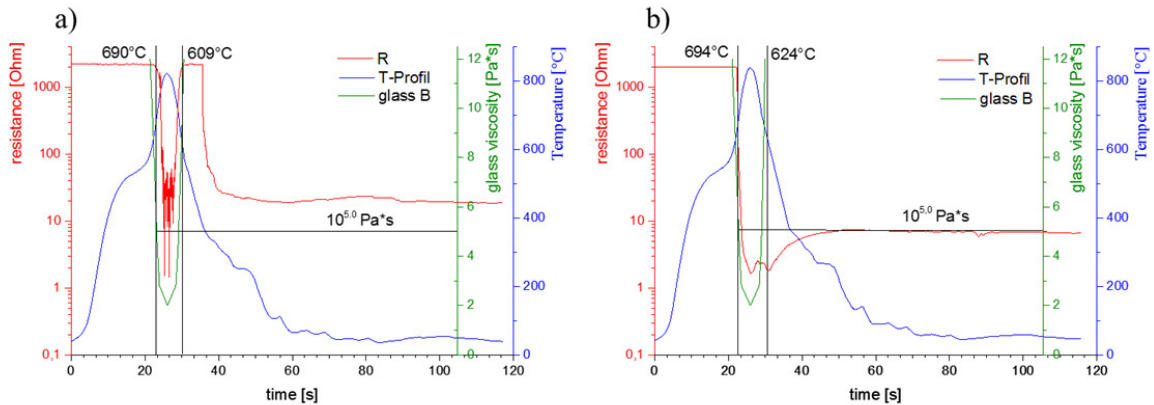


Figure 7: Contact resistance during as a function of time contact firing at 840°C of paste 4 (PbO free glass B, without Al – left hand side) and paste 6 (PbO free glass B, 7.5 Vol% Al – right hand side) as function of time. Red curve – contact resistance; blue curve – temperature; green – glass viscosity of glass B related to the temperature plot.

In Figure 7 the in-situ-contact resistance measurements of paste 4 (Figure 7a) and paste 6 (Figure 7b) during contact firing are shown. For paste 4 the resistance drop occurs at a temperature around 690°C corresponding to a glass viscosity of $10^{5.0}$ Pa*s (see Figure 1). Afterwards there is a scattering of the resistance in the peak temperature range. During cooling down the resistance increases and after a short while decreases again. The final value of ~19 Ohm reached after 100 s. A similar behavior was observed for this paste on a p-type wafer [8]. The resistance increase can be explained by glass re-solidification and related loss of electrical conductivity. The final drop is attributed to formation of Ag-precipitations and formation of percolating conductive paths during the cooling ramp. Paste 6 (Figure 7b) shows the first resistance drop also at about 690°C. This correlates well again with a glass viscosity of $10^{5.0}$ Pa*s as in case of the PbO-glass A, the addition of Al in the paste suppresses the scattering of the resistance in the peak firing range. This indicates a lower intensity of the reaction in the interface layer also in this case. The final resistance for paste 6 is 7 Ohm.

Paste 6 shows no increasing resistance during cool down. With Figure 5 in mind, this can be explained again with the thickness of the glass layer between silver and silicon. Adding Al to the paste, the glass layer gets thinner at some locations, and more Si-Ag-contact is formed. Comparing the final resistance at 100 s, in both silver-glass-compositions the addition of Al seems to improve the contact formation.

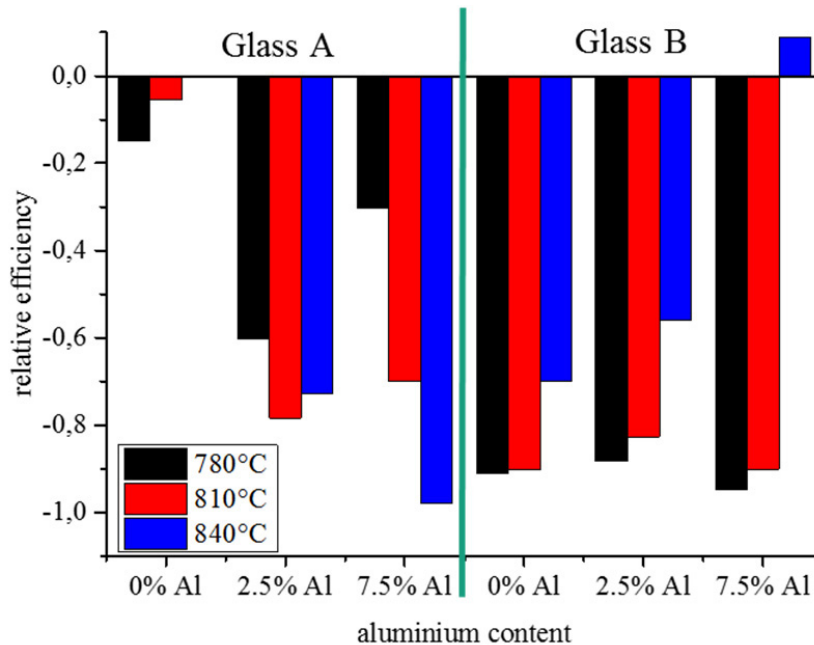


Figure 8: Relative efficiencies as a function of Al content of solar cells obtained by printing and firing the pastes according Table 1. Pastes with glass A – left hand side; pastes with glass B – right hand side.

In Figure 8 the relative efficiencies relating to paste 1 (fired at 840°C) are shown as a function of Al content of solar cells obtained for the pastes according Table 1. Different peak firing temperatures are shown as parameters.

On cell level, further important aspects for the contact formation (besides the formation of Ag precipitates) are emitter degradation or shunting hand [7, 17]. One should note that our model pastes are not optimized yet for all of these requirements, in contrast to commercial pastes. While the latter possibly contains further ingredients, our paste composition is chosen as simple as possible in order to study the major effects of the contact formation.

For pastes with glass A, with the addition of Al the efficiency is decreased for all firing temperatures. The paste with glass B shows an efficiency improvement with increasing firing temperature. The trend in the efficiency for different firing temperatures is encouraging that lead-free pastes for contacting p^+ -doped surfaces can be designed.

4. Conclusion

In this study, the contact formation of aluminum containing silver metallization pastes for boron emitters was investigated. Therefore, model pastes with varied glass composition (PbO-containing and PbO-free) and Al content were prepared. It is shown that the glass viscosity as well as the Al content have a strong influence on densification behavior of the pastes. With lower glass viscosity and lower Al content, the pastes can densify easier.

The interface layer between Ag and Si is also influenced by these two parameters. Using the low viscous glass A, the interface layer is rather thick. Using the high viscous glass B, the interface layer is very thin. For both systems the amount of silver precipitations in this layer is increased with peak firing temperature. Adding Al to the paste systems, the amorphous interface layer becomes even thinner and increasingly inhomogeneous. The glass amount in the finger bulk in the vicinity of the former Al grains is enriched.

N-PERT silicon solar cells were fabricated with the model pastes and electrically characterized. It was observed

that with glass A and addition of Al, the contact formation reaction is obviously too strong and yields an efficiency degradation. By contrast, the pastes with glass B and Al show with increasing temperature an increasing electrical performance. To conclude, the paste composition regarding glass and Al must be optimized in terms of Al content in relation to the glass viscosity.

Acknowledgements

At the IKTS, the author wants to thank to Nancy Hübner for paste preparation and measuring the in-situ-contact resistance.

At ISFH, this work was funded by the German Federal Ministry Economic Affairs and Energy (BMWi) under grant 0325480A (CHIP). We thank Sabine Kirstein, Anreas Klatt and Peter Giesel for their help with sample processing.

References

- [1] www.itrpv.net
- [2] M. A. Green et al., “19.1% efficient silicon solar cell”, *Appl. Phys. Lett.* 44, 1163 (1984); doi: 10.1063/1.94678.
- [3] D. Song, et. al., *Proc. of the 38th IEEE-PVSC 2012 Austin, TX, USA*, pp. 003004-003008.
- [4] V. D. Mihailetschi, et al., *Proc. of the 25th EU-PVSEC 2010, Valencia, Spain*, pp. 1446-1448.
- [5] K. K. Hong et al., “Role of PbO-Based Glass Frit in Ag Thick-Film Contact Formation for Crystalline Si Solar Cells”, *Met. Mater. Int.*, Vol. 15, No. 2 (2009), pp. 307-312, DOI: 10.1007/s12540-009-0307-1.
- [6] J. Y. Huh, “Effect of oxygen partial pressure on Ag crystallite formation at screen-printed Pb-free Ag contacts of Si solar cells”, *Materials Chemistry and Physics* 131 (2011) 113–119.
- [7] Z. G. Li, “Microstructural comparison of silicon solar cells’ front-side Ag contact and the evolution of current conduction mechanisms”, *J. Appl. Phys.* 110, 074304 (2011); doi: 10.1063/1.3642956.
- [8] G. Schubert, “Thick Film Metallisation of Crystalline Silicon Solar Cells”, PhD thesis, Konstanz, 2006.
- [9] R. Lago et al., *Prog. Photovolt: Res. Appl.* 2010; 18:20–27, DOI: 10.1002/pip.933.
- [10] H. Kerp, et. al., *Proc. of the 21st EU-PVSEC 2006, Dresden, Germany*, pp. 892-894.
- [11] M. König, et al., presented at 4th npv Workshop 2013, Chambéry, France.
- [12] L. Liang, et al., *IEEE Journal of PV* 4 (2), pp. 549-553.
- [13] M. Eberstein et al., “In-situ observations of glass frit related effects during the front side paste contact formation”, *Photovoltaic Specialist Conference (PVSC), 2014 IEEE 40th*, pp. 3463 – 3469.
- [14] M. Eberstein et al. “Sintering of glass matrix composites with small rigid inclusions”, *Journal of the European Ceramic Society* 29, 2009, 2469 – 2479.
- [15] K. D. Kim, “Electrical conductivity in Mixed-Alkali Aluminosilicate Melts”, *Journal American of Ceramic Society*, vol. 79 [9], pp. 2422 – 2428, 1996.
- [16] K. Reinhardt et al., “Observation of the contact formation of PV frontside pastes by in-situ contact resistance measurement”, *Energy Procedia*, PII: S1876610214012715, DOI: 10.1016/j.egypro.2014.08.047.
- [17] M. Eberstein et al., “Kinetic Aspects of the Contact Formation by Glass containing Silver Pastes”, *27th European Photovoltaic Solar Energy Conference and Exhibition (EUPVSEC), 2012*, 840 – 844.